

1 **SUPPLEMENTAL INFORMATION**

2 **A FOLDING TRANSITION UNDERLIES THE EMERGENCE**  
3 **OF MEMBRANE AFFINITY IN AMYLOID- $\beta$**

4 *Suman Nag<sup>†#@</sup>, Bidyut Sarkar<sup>†#</sup>, Muralidharan Chandrakesan<sup>‡</sup>, Rajiv Abhyankar<sup>†</sup>, Debanjan*  
5 *Bhowmik<sup>†</sup>, Mamata Kombrabail<sup>†</sup>, Sucheta Dandekar<sup>‡</sup>, Eitan Lerner<sup>§</sup>, Elisha Haas<sup>§</sup> and Sudipta Maiti<sup>†\*</sup>*

6 <sup>†</sup>Department of Chemical Sciences, Tata Institute of Fundamental Research, Homi Bhabha Road,  
7 Colaba, Mumbai 400005, India.

8 <sup>‡</sup>Department of Biochemistry, Seth G.S. Medical College and KEM Hospital, A.D. Marg, Parel,  
9 Mumbai 400012, India.

10 <sup>§</sup>The Mina and Everard Goodman Faculty of Life Sciences, Bar Ilan University, Ramat Gan 52900,  
11 Israel.

12 <sup>@</sup>Current address: B401, Beckman Center, Department of Biochemistry, Stanford School of Medicine,  
13 Stanford, CA-94025, USA.

14

15 \*Email: [maiti@tifr.res.in](mailto:maiti@tifr.res.in) (S.M)

16 # S.N and B.S contributed equally to this work.

17

## 18 **Materials, Reagent Preparation and Experimental Methodology**

### 19 **Materials**

20 All the 9-fluorenylmethoxycarbonyl (Fmoc) protected amino acids, Fmoc-Asp(EDANS)-OH, (2-  
21 (1H-7-Azabenzotriazol-1-yl)-1,1,3,3-tetramethyl uronium hexafluorophosphate methanaminium  
22 (HATU), O-benzotriazole-N,N,N',N'-tetramethyl uronium hexafluoro phosphate (HBTU), 1-  
23 hydroxybenzotriazole (HOBt), EDANS Novatag Resin, rink amide MBHA resin LL, triisopropylsilane  
24 (TIS) and N-(4-[4'-(Dimethylamino) phenylazo] benzyloxy) succinimide (DABCYL-OSu) were  
25 purchased from Merck (Schuchardt, Germany). Trifluoroacetic acid (TFA), N-methyl morpholine  
26 (NMM), N,N-dimethylformamide (DMF), acetic anhydride, tert-butyl methyl ether, acetonitrile,  
27 chloroform, uranyl acetate, di sodium hydrogen orthophosphate dihydrate ( $\text{Na}_2\text{HPO}_4 \cdot 2\text{H}_2\text{O}$ ) and  
28 potassium dihydrogen orthophosphate ( $\text{KH}_2\text{PO}_4$ ) were purchased from S.D. Fine Chem. Ltd. (Mumbai,  
29 India). Sodium chloride (NaCl) was obtained from Fisher Scientific (Mumbai, India). Potassium  
30 Chloride (KCl) and calcium chloride dihydrate ( $\text{CaCl}_2 \cdot 2\text{H}_2\text{O}$ ) were purchased from SRL (Mumbai,  
31 India). Magnesium sulphate ( $\text{MgSO}_4 \cdot 7\text{H}_2\text{O}$ ) was obtained from AnalaR, Glaxo laboratories (Mumbai,  
32 India). Hexafluoroisopropanol (HFIP), 4-(2-hydroxyethyl)-1-piperazineethanesulfonic acid (HEPES),  
33 1,8-diazabicyclo [5.4.0] undec-7-ene (DBU), dimethyl sulphoxide (DMSO), ploy-L-Lysine and  
34 dextrose were purchased from Sigma-Aldrich Inc. (St. Louis, MO, USA). *N,N*-Diisopropylethylamine  
35 (DIPEA), phenol, ethane dithiol (EDT), thioanisole and trifluoroethanol (TFE) were obtained from from  
36 Fluka (St. Louis, MO, USA). 5-(((2-iodoacetyl) amino) ethyl) amino) naphthalene-1-sulfonic acid  
37 (IAEDANS) was purchased from Molecular Probes (Eugene, Oregon, USA). Rhodamine labeled  
38 amyloid beta 40 (R-A $\beta_{40}$ ), N-terminal fluorescein labeled amyloid beta 40 (FL-A $\beta_{40}$ ) and C-terminal  
39 fluorescein labeled amyloid beta 40 (A $\beta_{40}$ -FL) were purchased from rPeptide (Bogart, GA, USA).  
40 Carbon-coated 100 mesh copper grids were purchased from Electron Microscopy Sciences (Hatfield,

41 PA, USA). PenStrep, Fetal Bovine Serum (FBS), DMEM-F12 media and Trypsin were purchased from  
42 Gibco (Grand Island, NY, USA).

### 43 **Reagent Preparation**

#### 44 **Buffer preparation**

45 The artificial cerebrospinal fluid (ACSF) buffer used for all the experiments consisted of 20  
46 mM Na<sub>2</sub>HPO<sub>4</sub>, 146 mM NaCl, 5.4 mM KCl, 1.8 mM CaCl<sub>2</sub>, 0.8 mM MgSO<sub>4</sub>, 0.4 mM KH<sub>2</sub>PO<sub>4</sub> and 5  
47 mM dextrose (pH adjusted to ~7.4). Modified Thomson's buffer (TB) (consisting of 20mM sodium  
48 HEPES, 146 mM NaCl, 5.4 mM KCl, 1.8 mM CaCl<sub>2</sub>, 0.8 mM MgSO<sub>4</sub>, 0.4 mM KH<sub>2</sub>PO<sub>4</sub>, 0.3 mM  
49 Na<sub>2</sub>HPO<sub>4</sub> and 5 mM dextrose; pH adjusted to ~7.4) was used for a few of the measurements. Most  
50 experiments were repeated in both buffers and no substantial difference was found in the measurements  
51 between the two buffers (though the solubility of A $\beta$  is lower in TB). All data reported here represent  
52 the average of all measurements, irrespective of the buffer used.

#### 53 **Peptide synthesis and purification**

54 In brief, A $\beta$ <sub>40</sub> was synthesized using Fmoc chemistry in an automated solid phase peptide  
55 synthesizer (PS3, Protein Technologies Inc. Tucson, AZ, USA). Use of rink amide MBHA resin for the  
56 synthesis yields peptide with carboxamide at the C-terminal. For each step of coupling, four-fold excess  
57 Fmoc amino acid was activated with equimolar HATU or HBTU and NMM (0.4M) in DMF. 4% DBU  
58 in DMF was used for deprotection of the Fmoc group. Finally, treatment with a mixture of 80% TFA +  
59 2.5% TIS + 5% water + 2.5% EDT + 5% thioanisole + 5% phenol for 4 hours was used to cleave the  
60 acid labile side chain protecting groups, while at the same time producing the free peptide in solution.  
61 The peptide was then concentrated under nitrogen flow and precipitated from the solution using tert-  
62 butyl methyl ether. The precipitate was washed thrice using the same ether followed by evaporation *in*  
63 *vacuo* to obtain the peptide in dry powder form.

64 For the A $\beta$ -EDANS (D-A $\beta$ <sub>40</sub>) peptide synthesis, instead of the rink amide resin, EDANS  
65 Novatag resin (resin loading 0.64mmol/g) was used, which had the fluorophore EDANS already  
66 attached to the resin. The synthesis proceeded from the C to the N-terminus with the first coupling  
67 between the carboxylic acid of C-terminal amino acid of A $\beta$  and the free secondary amine group of  
68 resin bound EDANS. This coupling was effected using the amino acid (4-fold excess) and HATU (4-  
69 fold excess) and DIPEA (8-fold excess) in DMF. Since the first coupling was not very efficient this step  
70 was repeated to get maximum coupling. The coupling efficiency was found to be ~70% using Fmoc  
71 detection.<sup>1</sup> Rest of the unreacted secondary amine sites of the resin bound EDANS was blocked by  
72 treatment with acetic anhydride. This step ensured that no unwanted chain of varying peptide length can  
73 grow. Rest of the coupling, peptide cleavage and recovery steps followed a method similar to that used  
74 for the unlabeled peptide. In this case the cleavage mixture cleaved the bond between EDANS and the  
75 resin yielding A $\beta$  with EDANS at the C-terminal of the peptide.

76 To prepare the FRET pair DABCYL-A $\beta$ -EDANS (DA-A $\beta$ <sub>40</sub>) peptide, DABCYL was attached to  
77 the N-terminus of the resin bound A $\beta$ -EDANS peptide using DABCYL-OSu (4-fold excess) in the  
78 presence of HOBt (2-fold excess) and DIPEA(4-fold excess) in DMF medium with constant stirring for  
79 24 hr. The cleavage and peptide recovery were performed as described earlier.

80 A $\beta$  with EDANS at the N-terminus of the peptide was prepared by using Fmoc-Aspartate with  
81 EDANS attached to the carboxyl side chain instead of regular Fmoc-Aspartate (Aspartate is the N-  
82 terminal amino acid).

83 The powdered crude peptides were dissolved in a 1:1 (vol/vol) mixture of HFIP and TFE and  
84 purified by reverse phase HPLC (Model: Prominence 20A, Shimadzu, Columbia, MD, USA) using a  
85 Kromasil C4 column (Kromasil, Bohus, Sweden). Water-acetonitrile (both containing 0.1% TFA)  
86 solvent gradient was used as for the elution. The purity of the peptides was verified by matrix assisted  
87 laser desorption ionization-time of flight mass spectrometry (MALDI-TOF MS, Model:TOF SPEC 2E,

88 Micromass, Manchester, England) or electrospray ionization mass spectrometry (ESI-MS, Finnigan  
89 LCQ Deca electrospray quadrupole ion trap mass spectrometer, Thermo Electron Corporation, San Jose,  
90 CA, U.S.A).

### 91 **Preparation of specimens with different sizes and their characterization**

92 The methods for preparing monomers and oligomers have been described by us earlier.<sup>2,3</sup>  
93 Briefly, peptides were dissolved in physiological buffer solutions at pH 7.4 and at 25°C. We prepared a  
94 mixed solution of 100  $\mu\text{M}$  of unlabeled  $\text{A}\beta_{40}$  along with 10  $\mu\text{M}$  of D- $\text{A}\beta_{40}$  or DA- $\text{A}\beta_{40}$  (as needed) and  
95 150 nM R- $\text{A}\beta_{40}$ , diluting from a stock solution prepared in water at pH 11. The time of this dilution  
96 (and consequent pH change to  $\sim 7.4$ ) was taken as the initial time point of the measurement.  $\text{A}\beta_{40}$  was  
97 supersaturated at these concentrations and started to aggregate, progressively producing large oligomers  
98 and insoluble precipitates. For preparing small oligomers, we centrifuged the solution at  $2000\times g$  for 20  
99 minutes after  $\sim 1$  day, and measured the size to ensure that the solution predominantly consisted of  
100 small oligomers. When this process was repeated for  $\sim 5$  days, only monomers were obtained, as  
101 reported earlier.<sup>2</sup> The particle sizes were measured by FCS (which used the rhodamine fluorescence)  
102 (Fig. S1a-f). We tested its ability of the large precipitates to form classic amyloid fibrils using  
103 transmission electron microscopy (Fig. S1g-h). The measurements for small oligomers and monomers  
104 were repeated for sub-saturated solutions (1-2  $\mu\text{M}$ ) without centrifugation. This initially yielded small  
105 oligomers, and after  $\sim 5$  days yielded monomers, also as reported earlier.<sup>2</sup> The small oligomeric and  
106 monomeric  $\text{A}\beta$  measurements were also separately repeated for fully labelled specimens at low  
107 concentrations (using pure D- $\text{A}\beta_{40}$  and pure R- $\text{A}\beta_{40}$ ). In each case, all sets of measurements gave very  
108 similar results (i.e. within the standard deviations of each other). Finally, the monomeric and the  
109 oligomeric solutions were tested for their affinity for RN46A cell membranes, by confocal microscopy  
110 (using a Zeiss LSM 710). We verified that the oligomers had strong affinity for the cell membranes at

111 250 nM concentration, while the monomers had very little affinity at the same concentration (Fig. S2),  
112 as found earlier.<sup>3</sup>

### 113 **Preparation of specimens with DA-A $\beta$ <sub>40</sub>**

114 It was difficult to obtain fully acceptor labeled DA-A $\beta$ <sub>40</sub> specimen in large quantities, and data  
115 reported for larger aggregates (which requires higher sample concentration) in this manuscript are from  
116 specimens with 64% acceptor labelling (as estimated by absorbance measurements, see 'Estimation of  
117 DABCYL labelling efficiency' in SI). In other words, a DA-A $\beta$ <sub>40</sub> molecule always had the donor  
118 (EDANS) at the C-terminal, but did not have the acceptor (DABCYL) in 36% of the cases. However we  
119 were successful in preparing a small amount of 100% acceptor labeled samples (see the mass spectrum  
120 in Fig. S3). We repeated the monomer and small oligomer FRET measurements with this sample (these  
121 measurements required small amounts of specimen). The data obtained using 100% and 64% DA-A $\beta$ <sub>40</sub>  
122 samples (after due correction, see section 'Correction of FRET efficiency' in SI) for the monomers and  
123 the small oligomers agree within experimental errors. Section 'Estimation of FRET efficiency for 100%  
124 and 64% acceptor labelled DA-A $\beta$ <sub>40</sub> peptides' in SI provides a full description of results comparing the  
125 64% and 100% DABCYL labelled DA-A $\beta$ <sub>40</sub> samples.

### 126 **Experimental Methodology**

#### 127 **Characterization of aggregates**

128 Co-aggregation of DA-A $\beta$ <sub>40</sub> with unlabeled A $\beta$ <sub>40</sub> was performed following a method described  
129 elsewhere.<sup>2,4</sup> FCS measurements were performed with an instrument constructed in-house.<sup>5</sup> Lifetime  
130 measurements of the solutions were performed by using the Time Correlated Single Photon Counting  
131 (TCSPC) method, with an instrument described elsewhere.<sup>6</sup> FCS data were fitted either with a discrete  
132 few-component diffusion model, and/or with a Maximum Entropy Method (MEM) based software  
133 written in house.<sup>7</sup> The FCS data were converted into hydrodynamic radii ( $R_h$ ) using rhodamine B ( $R_h =$   
134  $0.57 \text{ nm}^8$ ) as a calibrant. Further details are provided in the 'FCS measurements' section in SI.

### 135 **Estimation of DABCYL labelling efficiency**

136 The solid state peptide synthesis method ensured that the donor only sample (A $\beta$ <sub>40</sub>-EDANS or  
137 D-A $\beta$ <sub>40</sub>) was completely labelled by EDANS (5-((2-aminoethyl) amino) naphthalene-1-sulfonic acid) at  
138 the C-terminus. We calculated the percentage labelling of the acceptor DABCYL at the N-terminus of  
139 the donor-acceptor sample (DABCYL-A $\beta$ <sub>40</sub>-EDANS or DA-A $\beta$ <sub>40</sub>) by measuring the relative absorbance  
140 of the EDANS and DABCYL dyes attached to the peptide, and by using their molar extinction  
141 coefficients. The molar extinction coefficient for EDANS attached to the C-terminal of the peptide was  
142 measured to be 5300 M<sup>-1</sup> cm<sup>-1</sup> at 330 nm, which is close to values reported earlier (5700 M<sup>-1</sup> cm<sup>-1</sup> at 336  
143 nm for IAEDANS, as reported by the manufacturer, Molecular Probes). To measure the molar  
144 extinction coefficient of the peptide-attached DABCYL, we subjected a small amount of DA-A $\beta$ <sub>40</sub>  
145 specimen to multiple prolonged rounds of labelling with DABCYL-OSu under different solvent  
146 conditions (e.g in DMSO) for 10 days. This was continued until the purified DA-A $\beta$ <sub>40</sub> specimen showed  
147 no detectable trace of unlabeled specimen in the mass spectra (Fig. S3). This was used as a standard for  
148 a fully (100%) labeled DA-A $\beta$ <sub>40</sub> sample. Using this standard, we determined the extinction coefficient  
149 of the DABCYL attached to the N-terminus to be 6285 M<sup>-1</sup> cm<sup>-1</sup> at 450 nm. The ratio of the two  
150 absorbance peaks of the DA-A $\beta$ <sub>40</sub> specimen was measured and was compared to the ratio of the molar  
151 extinction coefficients at 450 nm and 330 nm. This yielded a labelling efficiency of 64% for most the  
152 specimens used for the experiments (unless otherwise stated). This implied that the nominal DA-A $\beta$ <sub>40</sub>  
153 sample had a mixture of D-A $\beta$ <sub>40</sub> and actual DA-A $\beta$ <sub>40</sub> in a ratio of ~ 1:2.

### 154 **Calculation of the FRET efficiency and inter-terminal distance distribution**

155 We calculated the efficiency of energy transfer (E), using the equation:

156

$$E = 1 - \frac{\tau_{da}}{\tau_d} \dots\dots\dots \text{Equation 1}$$

157 Where  $\tau_{da}$  and  $\tau_d$  are the mean lifetimes of the DA-A $\beta$ <sub>40</sub> and D-A $\beta$ <sub>40</sub> specimens respectively. Inter-  
158 terminal distance distributions and diffusion coefficients were calculated by global analysis of the

159 EDANS fluorescence decay curves using the model proposed by Beechem and Haas<sup>9</sup> (see 'Calculation  
160 of the inter-terminal distance distribution' in SI for details).

### 161 **Correction of FRET efficiency**

162 Most DA-Aβ<sub>40</sub> samples used in our experiments were only partially (64%) labelled with the  
163 acceptor (see 'Estimation of DABCYL labelling efficiency' in SI). Therefore any DA-Aβ<sub>40</sub> sample  
164 would have 36% peptide labelled with the donor only (D-Aβ<sub>40</sub>). This means that the apparent lifetime  
165 decay,  $\tau_{DA}^{app}$  from the DA-Aβ<sub>40</sub> sample would have contributions both from donor-only peptide ( $\tau_D$ ) and  
166 donor-acceptor labelled peptide ( $\tau_{DA}^{real}$ ), which would result in an incorrect estimate of FRET efficiency.  
167 This can be corrected if the fraction of labelling ( $x$ ) of the DA-Aβ<sub>40</sub> sample is known. In our case  $x$   
168 was 0.64. The apparent lifetime decay  $\tau_{DA}^{app}$  from the DA sample is given by

$$169 \tau_{DA}^{app} = x\tau_{DA}^{real} + (1-x)\tau_D \dots\dots\dots \text{Equation 2}$$

170 The apparent FRET efficiency is then calculated using Eq.3

$$171 E^{app} = 1 - \frac{\tau_{DA}^{app}}{\tau_D} \dots\dots\dots \text{Equation 3}$$

172 However the real FRET efficiency is given by

$$173 E^{real} = 1 - \frac{\tau_{DA}^{real}}{\tau_D} \dots\dots\dots \text{Equation 4}$$

174 Using equations 2, 3 and 4 it can be shown that

$$175 E^{real} = \frac{E^{app}}{x} \dots\dots\dots \text{Equation 5}$$

176 Eq. 5 was used to correct for FRET efficiencies obtained using 64% labelled DA-Aβ<sub>40</sub> samples. We  
177 note that the accuracy of this correction does not affect the relative FRET efficiencies of the different  
178 specimens.

### 179 **Calculation of the Förster distance for the EDANS-DABCYL pair**



180 The dependence of the FRET efficiency  $E$  on the separation between the donor and acceptor  
181 chromophores ( $R$ ) is given by

$$E = \frac{1}{1 + \left(\frac{R}{R_0}\right)^6} \dots\dots\dots \text{Equation 6}$$

183

184 where  $R_0$  is the Förster distance at which energy transfer efficiency is 50%.  $R_0$  can be calculated from  
185 the properties of the chromophores and the medium:

$$R_0^6 = \frac{0.529 * \kappa^2 * \phi_D * J}{N * n^4} \dots\dots\dots \text{Equation 7}$$

187 where  $R_0$  and the wavelength  $\lambda$  are in centimetres,  $\kappa^2$  describes the relative orientation of the  
188 fluorophores,  $\phi_D$  is the quantum yield of the donor,  $N$  is the Avogadro number, and  $n$  is the index of  
189 refraction of the medium.  $J$  is the spectral overlap integral, given by:

190

$$J = \frac{\int_0^\infty \phi(\lambda) * \varepsilon(\lambda) * \lambda^4 d\lambda}{\int_0^\infty \phi(\lambda) * d\lambda} \dots\dots\dots \text{Equation 8}$$

192

193 Here  $\phi(\lambda)$  is the area normalized donor emission spectrum and  $\varepsilon(\lambda)$  is of the acceptor absorbance  
194 spectrum ( $M^{-1} \text{ cm}^{-1}$ ). We measured the value of  $J$  for the EDANS-DABCYL pair attached to  $A\beta_{40}$  to be  
195  $\sim 1 * 10^{14} M^{-1} \text{ cm}^{-1} \text{ nm}^4$ . The value of the orientation factor ( $\kappa^2$ ) was taken to be 2/3 (for a freely rotating  
196 dye). This is a reasonable assumption, because the donor-acceptor pair is attached to the two termini of  
197 the peptide and should be relatively free to rotate. This was confirmed from the observed fast decay  
198 component ( $< 0.2 \text{ ns}$ ) of the rotational anisotropy of EDANS attached to the peptide (data not shown).  
199 Moreover, for fluorophores which have multiple transition dipole moments, the effect of the orientation  
200 factor goes down drastically.<sup>10</sup> We note that EDANS has multiple lifetimes and is thus expected to have  
201 multiple transition dipoles. Using the values of 1.39 for  $n$  inside a protein and the value of 0.27

202 for  $\phi_D$  (calibrated using standard fluorescein in pH 13), we obtained the Förster distance  $R_0$  (using Eq.7)  
203 to be 2.7 nm.

#### 204 **Co-aggregation studies**

205 We checked the effect of chromophore labeling on the aggregation properties of A $\beta_{40}$  by  
206 studying the co-aggregation of DA-A $\beta_{40}$  with unlabeled A $\beta_{40}$ . A mixed solution of 100  $\mu$ M of  
207 unlabeled A $\beta_{40}$  along with 10  $\mu$ M of DA-A $\beta_{40}$  was prepared in buffer, by diluting a stock solution  
208 prepared in water at pH 11. The absorbance at 260 nm, 330 nm and 450 nm were monitored for tyrosine  
209 (in the peptide), EDANS and DABCYL respectively. The initial absorbance values (at 10min) were  
210 normalized at these three wavelengths. We obtained similar absorbance values for all three at the end of  
211 aggregation (within a factor of two). This suggests that the dye labeled and unlabeled peptides co-  
212 aggregate and their properties are grossly similar. Further, we have tested that the labeled peptide was  
213 able to form classic amyloid fibrils (Fig. S1h). These suggest that chromophore attachment does not  
214 have a major effect on the aggregation properties of the peptide.

#### 215 **FCS measurements**

216 The homebuilt FCS set up used here was similar to that described elsewhere.<sup>5</sup> A collimated laser  
217 beam was focused into the sample volume using an apochromatic 60 $\times$  water immersion objective  
218 with NA of 1.2 (Olympus, America Inc, Center Valley, PA, USA). The emitted fluorescence was  
219 collected using the same objective and separated from the excitation beam by a dichroic mirror  
220 (Chroma, VT, USA). A 25  $\mu$ m core-diameter optical fiber was used as a confocal pinhole to reject the  
221 out of focus fluorescence. The fluorescence was filtered by a suitable emission filter (Chroma, VT,  
222 USA) before being detected by a single photon avalanche photodiode (APD, PerkinElmer Inc, Waltham,  
223 MA, USA). The data were processed using a hardware correlator card (ALV 5000E, ALV Laser,  
224 VmbH, Langen, Germany) which yielded the autocorrelation curves. These curves were analyzed using

225 a discrete diffusing component model using non-linear curve fitting with the Origin 7.5 software  
226 (OriginLab, Northampton, MA, USA). Alternatively, we also used the MEMFCS fitting routine to  
227 obtain a size distribution from the FCS data in a model-free manner.<sup>7</sup> The peak hydrodynamic radius, as  
228 determined by MEMFCS analysis (Fig. S1b) of the FCS data (Fig. S1a; data: red circles, fit: black,  
229 residuals: blue, auto-correlation: green) obtained from the monomeric R-A $\beta$ <sub>40</sub> was 0.8±0.1 nm and it  
230 remained constant with time. Single component fit of the same data produced a size of 0.8±0.1 nm for  
231 the monomers (Fig. S1b, dotted line). This is close to the value expected for the monomer,<sup>2</sup> and  
232 established that the specimen was predominantly monomeric. MEMFCS fitting (Fig. S1d) of the FCS  
233 data (Fig. S1c) for small oligomers showed the presence of particles with size of 1.8± 0.1 nm, which  
234 would be characteristic of an octamer (assuming a compact spherical shape). Of course, oligomers are  
235 unlikely to be completely spherical or fully compact (indeed, lack of compactness has been suggested  
236 before<sup>11</sup>), and this would imply that the number of monomers constituting the oligomer species is  
237 substantially less than 8. A discrete component fit yielded a size of 1.9±.1 nm for the oligomers (Fig.  
238 S1d, dotted line). Size distribution of the large oligomers obtained from the FCS measurements (Fig.  
239 S1e) showed their hydrodynamic radii to be approximately 22 nm (Fig. S1f). We note that the size  
240 determination for monomers and small oligomers are essentially repeats of experiments reported by us  
241 previously.<sup>2,12,13</sup>

## 242 **Lifetime measurements**

243 Lifetime measurements of the solutions were performed in a 2-mm path-length cuvette. The set  
244 up was described elsewhere.<sup>6</sup> Briefly, the excitation wavelength of 370 nm was obtained by generating  
245 the second harmonic of the 740 nm fundamental wavelength produced by a Nd:YAG-pumped titanium:  
246 sapphire laser (Spectra Physics, model No. 375B, Mountain View, CA) pulse-picked at 20 MHz. The  
247 emission monochromator was set to 490 nm. The fluorescence was collected at magic angle (54.7°) with  
248 respect to the excitation polarization. The instrument response function (IRF) was obtained at 370 nm,

249 using a very dilute colloidal suspension of milk powder. The width (full width at half maximum) of the  
250 IRF was  $<80$  ps. The decay was deconvoluted with respect to the IRF and analyzed using a sum of  
251 discrete exponentials.

### 252 **Estimation of FRET efficiency for 100% and 64% labelled DA-A $\beta_{40}$ peptides**

253 It was difficult to achieve full DABCYL labelling of the DA-A $\beta_{40}$  specimen, and all data (except  
254 as specifically mentioned) reported in the main manuscript is for specimens which are 64% DABCYL  
255 labeled (as estimated by absorbance measurements, see SI, 'Estimation of DABCYL labelling  
256 efficiency'). The FRET efficiency  $E$  reported in the manuscript was also obtained from the 64%  
257 DABCYL labeled DA-A $\beta_{40}$  samples which were then corrected as described in the SI section  
258 'Correction of FRET efficiency'. However, a 100% labeled DA-A $\beta_{40}$  specimen was also prepared (see  
259 the mass spectrum in the Fig. S3), and the measurements with monomers and oligomers (which require  
260 small concentrations) were repeated with this specimen. This was to verify that the results obtained with  
261 the 64% DA-A $\beta_{40}$  samples after correction agreed with 100% DA-A $\beta_{40}$  sample. The FRET efficiency  
262 estimates were very similar between 100% and 64% DABCYL labeled DA-A $\beta_{40}$  samples, as shown in  
263 Table S1.

#### 264 *For the monomers*

265 The lifetime of D-A $\beta_{40}$  monomers had a mean lifetime of  $8.9 \pm 0.6$  ns, whereas the 64%  
266 DABCYL labelled DA-A $\beta_{40}$  monomers had a mean lifetime of  $8.0 \pm 0.3$  ns. This yields an average  $E$  of  
267  $14.5 \pm 3.5\%$ . Accounting for partial labelling (see SI section 'Correction of FRET efficiency'), this yields  
268 a corrected  $E$  value of  $22.7 \pm 5.5\%$ . On the other hand, 100% labelled DA-A $\beta_{40}$  monomers yields a mean  
269 lifetime of  $5.6 \pm 0.3$  ns. This implies an average  $E$  of  $29.2 \pm 3.6\%$ , which is not significantly different.

#### 270 *For the Small Oligomers*

271 The lifetime of D-A $\beta_{40}$  small oligomer species had a mean value of  $10.0 \pm 0.7$  ns. The 64%  
272 DABCYL labelled DA-A $\beta_{40}$  for small oligomers had a mean lifetime of  $5.4 \pm 0.3$  ns, yielding a

273 corrected E value of  $71.1 \pm 4.7\%$ . On the other hand, the data obtained from 100% DABCYL labelled  
274 DA-A $\beta_{40}$  yields a mean life-time of  $3.5 \pm 0.3$  ns. This implies an E value of  $67.4 \pm 0.3\%$ , which is similar  
275 to that obtained from the 64% DABCYL labelled DA-A $\beta_{40}$  sample.

276 Together the monomer and the small oligomer data shows that the corrected FRET efficiency  
277 calculated from the 64% DABCYL labelled DA-A $\beta_{40}$  samples and the FRET efficiency calculated from  
278 the 100% DABCYL labelled DA-A $\beta_{40}$  samples match within experimental errors.

### 279 Calculation of the inter-terminal distance distribution

280 Inter-terminal distance distributions and self-diffusion coefficients were calculated by global  
281 analysis of the EDANS fluorescence decay curves of corresponding D-A $\beta_{40}$  and the DA-A $\beta_{40}$   
282 specimens. All DA-A $\beta_{40}$  donor fluorescence decay curves were globally fitted to the following model.<sup>9</sup>  
283 Equation 9 depicts the spatial and temporal survival probability of a donor electron in the electronic  
284 excited state in the presence of an acceptor which is at distances characterized by state j, which denotes  
285 one of the two states.

$$286 \quad \frac{\partial \bar{N}_j^*(r,t)}{\partial t} = - \left\{ \sum_{i=1}^n \frac{\alpha_i}{\tau_i} \left[ 1 + \left( \frac{R_0}{r} \right)^6 \right] \right\} \bar{N}_j^*(r,t) + \frac{1}{N_{0j}(r)} \frac{\partial}{\partial r} \left[ N_{0j}(r) \text{Diff}_j(r) \frac{\partial \bar{N}_j^*(r,t)}{\partial r} \right] \dots \dots \text{Equation 9}$$

$$287 \quad [D^*]_j(t) = \text{Norm} \cdot \int_a^{r_{\max}} N_j^*(r,t) dr; \bar{N}_j^*(r,t) = \frac{N_j^*(r,t)}{N_{0j}(r)}; N_{0j}(r) = N_j^*(r, t=0); j = 1,2$$

288 Here  $r$  is the inter-fluorophore distance,  $t$  is the time after excitation moment,  $\text{Diff}(r)$  is the inter-  
289 fluorophore self diffusion coefficient during excited state survival taken here as a constant over all inter-  
290 fluorophore distances,  $N_0(r)$  represents the equilibrium distribution of distances,  $N^*(r,t)$  represents the  
291 donor excited-state spatiotemporal survival probability and  $\bar{N}^*(r,t)$  equals  $N^*(r,t)$  normalized to the  
292 equilibrium distance distribution,  $R_0$  is the Förster radius and  $\tau_i$  is the  $i^{\text{th}}$  lifetime component with

293 normalized amplitude of  $\alpha_i$ . The integral over all available distances,  $[D^*](t)$ , represents the calculated  
294 donor fluorescence decay law for a given equilibrium distance distribution.

295 For this analysis, we used a skewed Gaussian model for the distribution of each population (Eq.  
296 10),

$$297 N_0(r) = c \cdot 4\pi r^2 e^{-b(r-a)^2} \dots\dots\dots \text{Equation 10}$$

298 Here  $a$  is a parameter representing the mean distance,  $b$  represents the reciprocal of the width and  $c$  is  
299 the normalization factor.

300 The analysis was performed for each population. The calculated donor fluorescence decay law  
301 for each population,  $[D^*]_j(t)$  was weighted by their equilibrium fraction,  $x_j$  and summed. The  
302 convolution of the resultant fluorescence decay law with the instrument response function  $IRF(t)$  is the  
303 calculated donor fluorescence decay (Eq. 11).

$$304 I_{DA}(t) = IRF(t) \otimes \left\{ \sum_{j=1}^2 x_j [D^*]_j(t) \right\} \dots\dots\dots \text{Equation 11}$$

305 For monomers only a single population was used. For small oligomers, two distance  
306 distributions were used: one for the monomer fraction and the other for the small oligomer fraction. The  
307 monomer distance distribution parameters were globally shared.

308 All D- $\text{A}\beta_{40}$  donor fluorescence decay curves were also globally fitted to the convolution of the  
309 instrument response function with the weighted sum of exponentials used in Eq. 9 (see Eq. 12 below).

$$310 I_D(t) = IRF(t) \otimes \left\{ \sum_{i=1}^n \alpha_i e^{-\frac{t}{\tau_i}} \right\} \dots\dots\dots \text{Equation 12}$$

311 The data from 64% labelled sample was also analysed for all the four species. This analysis is  
312 presented in Fig. 1f and it shows strong similarities with the analysis made from the 100% acceptor  
313 labelled samples for monomers and small oligomers (Fig. 1f, Inset). The data also shows that the large

314 oligomers and the fibrils have distance distributions which are very similar to those of the small  
315 oligomers. However, we note that the incomplete labelling makes the fitting less reliable.

### 316 **Transmission electron microscopy**

317 200  $\mu\text{M}$   $\text{A}\beta_{40}$  (or DA- $\text{A}\beta_{40}$ ) solution was prepared in aqueous buffer and incubated for 7 days at  
318 room temperature. After 7 days, 10  $\mu\text{l}$  of the solution was placed on a carbon-coated 100 mesh copper  
319 grid and allowed to be adsorbed for 2 minutes. The extra solution was removed with a filter paper,  
320 followed by three cycles of mild washing with double distilled water. For staining, a drop of 0.1 %  
321 uranyl acetate was added to the grid and left for 5 min. The grid was dried under an infrared lamp after  
322 removing the excess uranyl acetate solution using a filter paper. The samples were then examined with a  
323 transmission electron microscope (LIBRA 120, EFTEM, Carl Zeiss, Germany). The fibrils formed by  
324 DA- $\text{A}\beta_{40}$  (Fig. S1h) were mostly similar to that formed by unlabeled  $\text{A}\beta_{40}$  (Fig. S1g).

### 325 **Solvent accessibility of the termini**

326 The solvent accessibility of fluorescein dye attached to the different termini of the  $\text{A}\beta$  peptide  
327 was assessed by collisional quenching of the fluorophore by KI in a home-built microscopic TCSPC  
328 setup. The setup was similar to the FCS set up described earlier. Briefly, we used a 490 nm pulsed  
329 diode laser (PicoQuant, Germany) for excitation and single photon avalanche photodiode (Micro Photon  
330 Devices, Italy) for detection, along with appropriate dichroic mirror and emission filters. This yielded  
331 simultaneous FCS and TCSPC measurements. The data were recorded with PicoHarp 300 and analysed  
332 with Symphotime (Picoquant, Germany). We performed fluorescence lifetime measurements on 1  $\mu\text{M}$   
333 monomeric (or oligomeric) solution of  $\text{A}\beta_{40}$  labelled fluorescein at the N-terminal (FL- $\text{A}\beta_{40}$ ) or at the  
334 C-terminal ( $\text{A}\beta_{40}$ -FL) in ACSF in a home-made glass bottomed Petri dish. The measurements were  
335 repeated following gradual addition of KI (from 1M stock solution in water) varying from 0 to 50 mM  
336 of KI. Fibrils were prepared by aggregating 100  $\mu\text{M}$   $\text{A}\beta_{40}$  doped with 1  $\mu\text{M}$  FL- $\text{A}\beta_{40}$  (or  $\text{A}\beta_{40}$ -Fl) in

337 ACSF for 3 days. The fibrils were precipitated, and the precipitates were re-suspended in ACSF and  
338 mixed well in vortex shaker before measurements. The fibrils from the solution tend to settle at the  
339 bottom of Petri dish, so the measurements were performed near the surface with slow mixing of the  
340 solution away from the focus (without generation of bubbles which can scatter light). The fluorescence  
341 lifetime were analysed for 2-component exponential decay. The mean lifetime values were used to  
342 generate Stern-Volmer plots (Fig. S5), which yield the bi-molecular quenching rate constants (Fig. 2).

### 343 **Membrane affinity studies**

344 RN46A cells were cultured in Dulbecco's modified Eagle's medium (DMEM)-F12 (1:1)  
345 supplemented with 10% FBS, 50units/ml Penicillin and 50  $\mu$ g/ml Streptomycin at 37°C under  
346 humidified air containing 5% CO<sub>2</sub> in T-25 canted-neck flasks. For membrane binding studies the cells  
347 were cultured in home-made cover slip-bottomed Petri dish coated with poly-L-Lysine (0.1mg/ml). The  
348 initially imaged the cells for their autofluorescence ( $\lambda_{\text{ex}} = 543$  nm,  $\lambda_{\text{em}} = 550-700$  nm) in a confocal  
349 microscope (LSM-710, Carl Zeiss, Germany). Following 30 min of incubation with sham (TB), 250 nM  
350 monomeric or oligomeric R-A $\beta$ <sub>40</sub> solutions the dishes were washed with buffer and imaged again. We  
351 analyzed the brightness of the membrane region of the cells (at the brightest Z-position) after  
352 subtraction of the non-cell background, using ImageJ (open source software, available from the website  
353 <http://rsbweb.nih.gov/ij/>). Fig. S2a, S2b and S2c show three sets of cells at zero-time. Fig. S2d, S2e and  
354 S2f show the same cells after 30 min of treatment with sham, R-A $\beta$ <sub>42</sub> monomers (250 nM) and  
355 oligomers (250 nM) respectively. The membranes of the cells incubated with the oligomers brightened  
356 up considerably ( $\sim 25\times$ , Fig. S2c vs. Fig. S2f), while monomers hardly caused any change (Fig. S2b vs.  
357 Fig. S2e). We note that the membrane binding results shown here are repeats of experiments reported  
358 earlier by us.<sup>2,3</sup>

359



360 **References**

- 361 (1) M. Gude; J. Ryf and P. D. White, *Lett Pept Sci*, 2002, **9**, 203-206.
- 362 (2) S. Nag; B. Sarkar; A. Bandyopadhyay; B. Sahoo; V. K. Sreenivasan; M. Kombrabail; C.  
363 Muralidharan and S. Maiti, *J Biol Chem*, 2011, **286**, 13827-13833.
- 364 (3) B. Sarkar; A. K. Das and S. Maiti, *Frontiers in Physiology*, 2013, **4**.
- 365 (4) P. Sengupta; K. Garai; B. Sahoo; Y. Shi; D. J. Callaway and S. Maiti, *Biochemistry*, 2003, **42**,  
366 10506-10513.
- 367 (5) P. Sengupta; J. Balaji and S. Maiti, *Methods*, 2002, **27**, 374-387.
- 368 (6) A. Jha; J. B. Udgaonkar and G. Krishnamoorthy, *J Mol Biol*, 2009, **393**, 735-752.
- 369 (7) P. Sengupta; K. Garai; J. Balaji; N. Periasamy and S. Maiti, *Biophys J*, 2003, **84**, 1977-1984.
- 370 (8) C. T. Culbertson; S. C. Jacobson and J. Michael Ramsey, *Talanta*, 2002, **56**, 365-373.
- 371 (9) J. M. Beechem and E. Haas, *Biophys J*, 1989, **55**, 1225-1236.
- 372 (10) E. Haas; E. Katchalski-Katzir and I. Z. Steinberg, *Biochemistry*, 1978, **17**, 5064-5070.
- 373 (11) K. Ono; M. M. Condrón and D. B. Teplow, *Proc Natl Acad Sci U S A*, 2009, **106**, 14745-14750.
- 374 (12) K. Garai; B. Sahoo; S. K. Kaushalya; R. Desai and S. Maiti, *Biochemistry*, 2007, **46**, 10655-  
375 10663.
- 376 (13) B. Sahoo; J. Balaji; S. Nag; S. K. Kaushalya and S. Maiti, *J Chem Phys*, 2008, **129**, 075103.

377

378

379

380

381

382

383 **Figure legend**

384 **Figure S1. Size and morphology of A $\beta$  monomers and aggregates: (a, c, e)** Size of A $\beta$ <sub>40</sub> monomers  
385 **(a)** small oligomers **(c)** and large oligomers **(e)** determined by MEMFCS fit (black) to autocorrelation  
386 curves (red circles) obtained for Fluorescence correlation spectroscopy of rhodamine labeled A $\beta$ <sub>40</sub>;  
387 residuals (Res): blue, 10 times magnified and autocorrelation of residuals (AC): green. **(b), (d)** and **(f)**  
388 show the size distribution obtained from the MEMFCS fit (circles) and discrete component fit (dotted  
389 vertical lines) to the data in **(a), (c)** and **(e)** respectively. **(g, h)** Negatively stained Transmission Electron  
390 Microscopy image of fibrils obtained by maturing 200  $\mu$ M of A $\beta$ <sub>40</sub> **(g)** and 200  $\mu$ M of DA-A $\beta$ <sub>40</sub> **(h)** in  
391 buffer for 7 days; Scale bar = 500 nm.

392 **Figure S2. Binding of A $\beta$ <sub>40</sub> monomers and oligomers to RN46A cell membranes:** confocal images  
393 of RN46A cells at 0 min **(a, b, c)** and after 30 min **(d, e, f)** of incubation with buffer **(a, d)**, 250 nM of  
394 monomeric R-A $\beta$ <sub>40</sub> **(b, e)**, and 250 nM of small oligomeric R-A $\beta$ <sub>40</sub> **(c, f)**. Intensity is false color coded.  
395 Scale bar = 20 $\mu$ m. We note that the data shown here are repeats of experiments reported earlier by us.<sup>2,3</sup>

396

397 **Figure S3. Mass spectrum of FRET-labeled A $\beta$ <sub>40</sub>:** The multiply charged species of the 100% donor-  
398 acceptor labeled A $\beta$ <sub>40</sub> (DA-A $\beta$ <sub>40</sub>) sample are marked in the spectrum. **Inset:** Data after deconvolution  
399 shows only 100% labeled DA-A $\beta$ <sub>40</sub> (Expected mass: 4829). The donor only labeled A $\beta$ <sub>40</sub> (D-A $\beta$ <sub>40</sub>) has  
400 a mass of 4575, which is absent.).

401 **Figure S4. Stern-Volmer plots for the termini quenching of A $\beta$ <sub>40</sub>:** for monomers **(a)**, oligomers **(b)**  
402 and fibrils **(c)** determined from fluorescence lifetime of fluorescein labeled at the N-terminus (black  
403 squares) and C-terminus (red circles) of A $\beta$ <sub>40</sub> respectively.

404

405

406

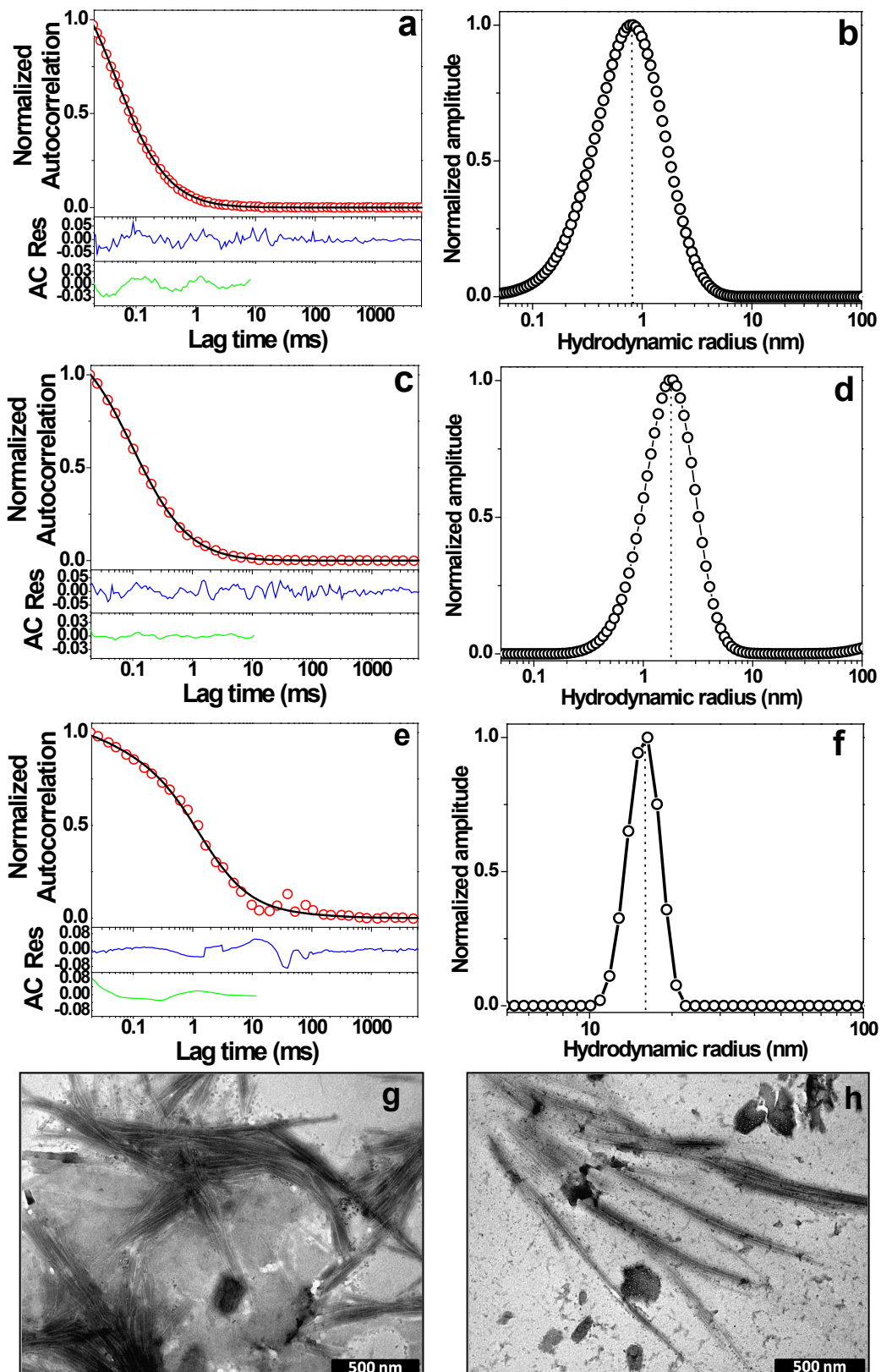


Figure S1

407

408

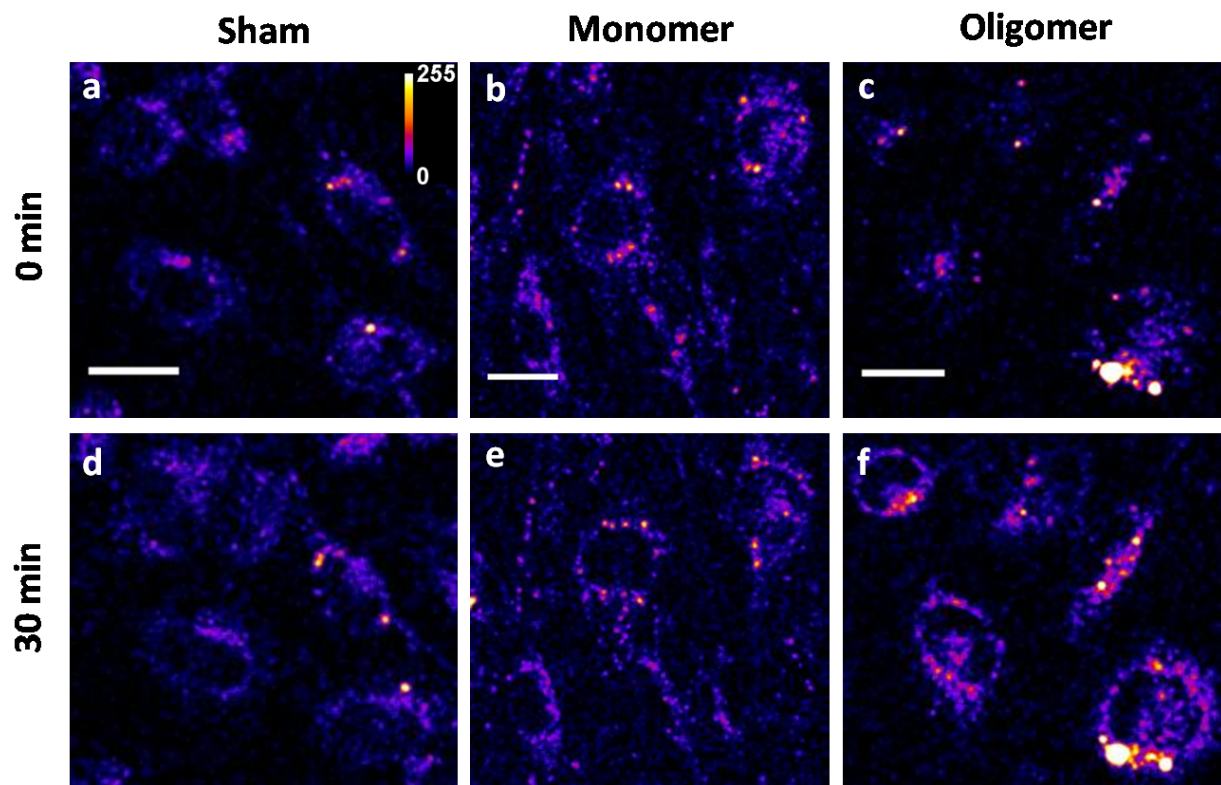


Figure S2

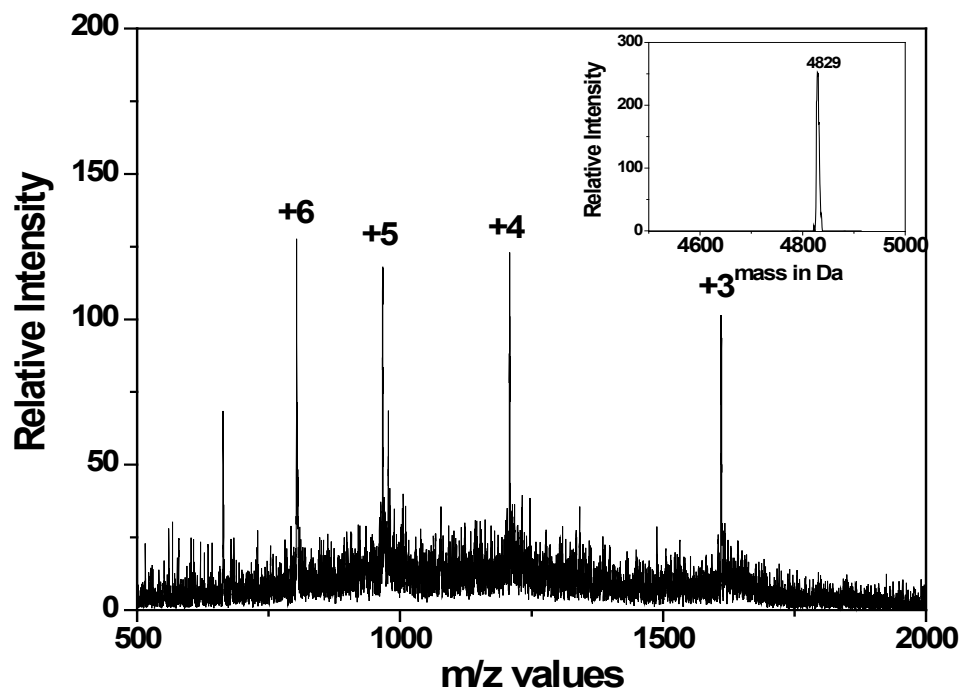


Figure S3

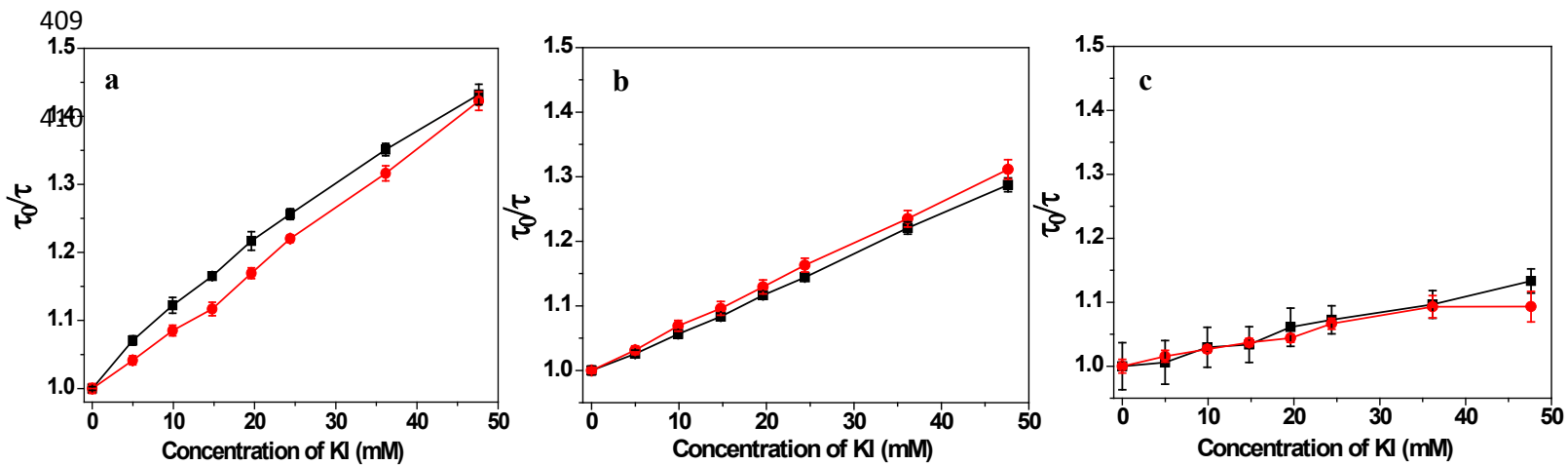


Figure S4

**Table S1. Lifetime components for different species obtained from multi-exponential fits**

Sample	Type	$\tau_1$	$a_1$	$\tau_2$	$a_2$	$\tau_3$	$a_3$	$\tau_4$	$a_4$	$\tau_m$	E%
M	D-A $\beta_{40}$	0.42±0.09	0.19±0.05	3.2±0.3	0.13±0.05	12.5±0.8	0.7±0.1	-	-	8.9 ±0.6	-
M	DA-A $\beta_{40}$	0.41±0.12	0.22±0.03	2.8±0.3	0.11±0.01	11.3±0.1	0.67±0.02	-	-	8.0±0.3	22.7±5.5
M	DA-A $\beta_{40}$ (100%)	0.29±0.06	0.40±0.09	2.4±1.2	0.18±0.03	12.0±0.3	0.42±0.06	-	-	5.6±0.3	29.2±3.6
SO	D-A $\beta_{40}$	0.62±0.12	0.17±0.04	3.9±0.4	0.23±0.03	14.7±1.0	0.60±0.04	-	-	10.0±0.7	-
SO	DA-A $\beta_{40}$	0.45±0.05	0.37±0.05	2.3±0.3	0.23±0.02	11.4±0.6	0.41±0.04	-	-	5.4±0.3	71.4±4.7
SO	DA-A $\beta_{40}$ (100%)	0.25±0.03	0.43±0.06	1.5±0.3	0.26±0.03	9.15±0.03	0.33±0.03	-	-	3.5±0.3	67.4±0.3
LO	D-A $\beta_{40}$	10.50±0.26	0.08±0.01	3.4±0.7	0.19±0.02	15.2±0.5	0.74±0.02	-	-	12.1±0.5	-
LO	DA-A $\beta_{40}$	0.34±0.10	0.23±0.01	2.2±0.3	0.22±0.04	11.5±0.3	0.56±0.04	-	-	7.0±0.7	65.0±10.0
PPT	D-A $\beta_{40}$	1.20±0.34	0.22±0.13	11.0±1.0	0.46±0.07	22.1±1.7	0.30±0.07	-	-	12.1±1.0	-
PPT	DA-A $\beta_{40}$	0.30±0.27	0.20±0.07	1.5±0.3	0.35±0.07	8.0±0.7	0.25±0.07	19.0±1.3	0.25±0.07	7.2±0.5	63.0±7.8

Monomer, M; small oligomers, SO; large oligomers, LO; and precipitate, PPT for donor only (D-A $\beta_{40}$ ) and donor-acceptor labeled specimens (DA-A $\beta_{40}$ ).  $\tau_i$  ( $i=1, 2, 3, 4$ ) are the different lifetime components with corresponding amplitudes  $a_i$ , and  $\tau_m$  is the mean lifetime. E% are the corrected percentage FRET efficiencies calculated from the mean lifetime and the estimated labeling efficiency values. For M and SO, DA-A $\beta_{40}$  (100%) shows results from 100% acceptor labeled specimens. 64% acceptor labeled DA-A $\beta_{40}$  specimens were used for the rest of the experiments.

**Table S2. Biophysical parameters for different species obtained from fitting of the FRET data to a skewed Gaussian model:**

<b>Monomer inter-terminal Distance<sup>a</sup> (Å)</b>	<b>Monomer FWHM<sup>b</sup> (Å)</b>	<b>Small Oligomers inter-terminal Distance (Å)</b>	<b>Small Oligomers FWHM (Å)</b>	<b>Monomer Inter-terminal Diffusion Coefficient (Å<sup>2</sup>/ns)</b>	<b>Small Oligomers Inter-terminal Diffusion Coefficient (Å<sup>2</sup>/ns)</b>	<b>Fraction of Monomers in Small Oligomers Measurement</b>
56.1 (56.1-61.4)	63.8 (63.0-69.9)	19.9 (19.4-21.0)	23.9 (19.7-23.9)	13.7 (13.0-39.1)	1.9 (1.0-4.9)	0.27 (0.18-0.33)

<sup>a</sup> – The most probable distance according to the distance distribution.

<sup>b</sup> - Full Width at Half of Maximum of the distance distribution.